P4R.9 DESIGN AND TEST OF AN OPERATIONAL TRIPLE-PRT DOPPLER SCHEME FOR THE FRENCH RADAR NETWORK

Pierre Tabary[1]

[1]Meteo-France, DSO, Centre de Météorologie Radar, Trappes, France

1. INTRODUCTION

Staggered PRT schemes have recently received much attention (Zrnic 1977; Zrnic and Mahapatra 1985; Gray et al. 1989; Sachidananda and Zrnic 2002; Torres et al. 2004; Tabary et al. 2005) for their ability to solve the long-lasting range – velocity dilemma. Due to the interleaving of the radar pulses, the various velocities of multiple-PRT schemes correspond exactly to the same volume of atmosphere. Therefore, unlike multiple-PRF schemes, they do not suffer from high wind-shear or rapid antenna rotation. Moreover, Zrnic and Sachidananda (2002) have shown recently how to overcome the main drawback of staggered PRT, namely the impossibility to perform spectral processing of such sequences, and a staggered PRT will soon be adopted for the NEXRAD radars (Zrnic and Zahrai 2003).

Tabary et al. (2005) presented an evaluation of a dual-PRT scheme that has been implemented operationally on a C-band radar of the French network. The two PRF that were used were very low (around 333 Hz) and very close to each other (the ratio of Nyquist velocities was about 6/7). The extended Nyquist velocity was about 30 m.s-1. In July 2004, the dual-PRT scheme was replaced by a triple-PRT scheme with the main objective to 1) improve the de-aliasing success rate and 2) further extend the resulting Nyquist velocity. The three PRF, PRF_1, PRF_2 and PRF_3, were set - somewhat arbitrarily - respectively to 379, 325 and 303 Hz. The three associated Nyquist velocities, V_{N1}, V_{N2} and V_{N3}, are respectively equal to 5.05, 4.33 and 4.04 $m.s^{-1}$. The ratios V_{N2}/V_{N1} andV_{N3}/V_{N1} are respectively equal to 6/7 and 4/5, *i e* very close to unity. Given the fact that Nyquist velocities are expressed in terms of ratio of prime integers, the extended Nyquist velocity V_N is easy to compute and reads (see the analysis by Torres et al. (2004)) :

$$V_N = \mathrm{lcm}(6,4).V_{N1} = 12.V_{N1} = 60.6 \text{ m.s}^{-1}, \quad (1)$$

where lcm stands for least common multiple. Three dual-PRT velocities can be computed from the triplet (V_1, V_2, V_3) : V_{12}, V_{13} and V_{23}. Given the values of the ratios (V_{N2} / V_{N1} = 6/7; V_{N3} / V_{N1} = 4/5 and V_{N3} / V_{N2} = 14/15), the associated Nyquist velocities of the three dual-PRT sub-schemes can be computed as follows :

$$V_{N12} = 6.V_{N1} = 30.3 \text{ m.s-1} \quad (2)$$
$$V_{N13} = 4.\ V_{N1} = 20.2 \text{ m.s-1} \quad (3)$$
$$V_{N23} = 14.V_{N2} = 60.6 \text{ m.s-1}. \quad (4)$$

One month of data (August 2004) comprising a mixture of convective, stratiform and clear-air situations, has been analyzed in order to evaluate the performances of the triple-PRT scheme. Section 2 presents the radar characteristics and the radar data processing. Section 3 is devoted to the quantitative evaluation of the triple-PRT scheme. In Section 4, a simulation “à la Zrnic” (Zrnic 1977) of I and Q time series is used to reproduce the observed error histograms in a Monte-Carlo approach. The same simulation tool is used to extensively compare dual- versus triple-PRT schemes and to rank them in 2D diagrams according to 1) the de-aliasing success rate and 2) the extended Nyquist velocity. Results are summarized in section 5

2. PRESENTATION OF THE RADAR AND THE RADAR DATA PROCESSING

The Trappes radar is a C-band radar equipped with a coaxial magnetron. The peak power, pulse width and gate spacing are respectively equal to 250 kW, 2 μs and 240 m. Tabary et al. (2005) have described the hardware and software modifications that had to be done to allow Doppler processing. Special emphasis was laid on the clear-air detection capability of the radar by adding an additional low-noise linear receiver to the system. It has been shown that low-level radial velocity measurements can be obtained 95% of the time in warm season. Over the period analyzed in the present paper (August 2004), the scan strategy of the radar consisted in 4 rounds per 5 minutes (antenna rotation rate of about 5°/s). Two elevation angles were repeated every 5 minutes (0.4 and 1.5°) because they are used to produce the operational Quantitative Precipitation Estimates (QPE), the update frequency of which is 5 minutes, and the remaining two elevation angles of the 5 minute cycle were changed from one cycle to the following one. A complete volume with 8 elevation angles was obtained over 15 minutes.

The velocities at lag PRT_1, PRT_2 and PRT_3 are estimated classically with the Pulse-Pair technique. The complex correlations are calculated for each pulse pair and each range gate and then projected directly onto a Cartesian grid. The size and resolution of that grid are respectively equal to 512x512 km_ and 1km_. The consequence of that technique is that the number of estimates per pixel varies according to the distance. On average, given the antenna rotation rate, the mean PRF and the gate spacing, this leads to about 1000 (resp. 100) non-independent pulse-pair estimates for each

* *Corresponding author address:* Pierre Tabary, Centre de Météorologie Radar, DSO, Météo France, 7 rue Teisserenc-de-Bort 78195, Trappes, France; email: pierre.tabary@meteo.fr

velocity for a 1 km_ pixel located at 10 (resp. 100) km from the radar. The de-aliasing procedure is the following:

- generate the set of the 12 possible aliases of V_1 within the extended Nyquist interval $[-V_N;V_N]$: $V_{TEST} = V_1 \pm 2.k.V_{N1}$;
- for each alias, compute the difference, *modulo* $2V_{N2}$, with the velocity at lag PRT_2 : $\Delta_2=(V_{N2}/\pi).\arg[e^{j\pi(VTEST-V2)/VN2}]$, where arg(X) stands for the argument of the complex number X;
- for each alias, compute the difference, *modulo* $2V_{N3}$, with the velocity at lag PRT_3 : $\Delta_3=(V_{N3}/\pi).\arg[e^{j\pi(VTEST-V3)/VN3}]$;
- the alias that is chosen (k_{best}) is the one that leads to the smallest Root Mean Square error : $RMS_V = \sqrt{0.5(\Delta_2\_+\Delta_3\_)}$;
- the de-aliased velocity V_{123} is then simply obtained as : $V_{123} = V_1+2.k_{best}.V_{N1}$.

It has been shown (Zrnic 1977) that the higher the PRT is, the smaller is the variance of the estimated velocity. In the present case, de-aliasing is done using the velocity at the shorter lag PRT_1. This is in part motivated by computing time considerations: indeed, if V_3 were used, then it is not 12 but 15 aliases that should be tested. Besides, it should be recalled here that the three PRF are very close to each other (303, 325 and 379 Hz) so there shouldn't be a big difference in the variance of the three velocity estimations. The de-aliasing procedure can be further extended for any number of different PRT. Although the de-aliasing rules proposed by Torres et al. (2004) are very attractive in that they are very computationally un-expensive, it would be probably complicated to generalize them to a triple-PRT scheme. The RMS_V corresponding to the best alias is also a measure of the consensus between the three aliased velocities and, consequently, a good indicator of the quality of the de-aliased velocity. In absence of noise, that quantity should always be zero.
In operations, Cartesian PPIs of reflectivity, pulse-to-pulse reflectivity fluctuations (parameter called σ), V_1, V_2, V_3 and V_{123} are generated in real-time and stored. RMS_V can be re-computed a posteriori from V_1, V_2 and V_3. So far, PPIs of the Doppler spectrum width have not been produced even though standard formula are available (Zrnic 1977).

Figure 1 shows the reflectivity (top), velocity at lag PRT_1 (middle) and de-aliased velocity (bottom) for an elevation angle of 1.5° during a stratiform rain event with strong winds (17 December 2004 10.00 UTC). All PPIs have the same size and resolution : 512x512 km_ and 1 km_. Comparing the middle and bottom fields shows clearly that the de-aliasing procedure is quite efficient. Some erroneous pixels however are clearly visible on the bottom image. They correspond to de-aliasing failures. In the next section we document their statistical distributions.

3. QUANTITATIVE ASSESSMENT OF THE TRIPLE-PRT SCHEME

The quantitative assessment of the scheme requires a reference velocity field. Unfortunately, no instrument is able to provide information on the wind field with the same space-time resolution and with the same geometry as a Doppler radar. Radio-sounding or wind profiler data could have been used but they only provide vertical profiles, they are not necessarily co-located with the radars, they have their own instrumental errors. Therefore, we decided instead to generate the reference radial velocity field "internally" as follows :

- compute for each pixel of each PPI the de-aliased radial velocity V_{123} from the triplet V_1, V_2, V_3. Measurements that have a Signal-to-Nose Ratio less than 3 dB are flagged out;
- flag out all radial velocities V_{123} that are less than 1 $m.s^{-1}$ (in absolute value) in order to remove cluttered pixels. That criterion is very drastic and clearly removes the zero radial-velocity pixels in precipitation areas but at least the remaining pixels are by no means affected by ground-clutter;
- apply a 5x5 km_ median filter to the remaining data. The resulting value ($V_{filtered}$) is validated only if all 25 pixels in the neighborhood were actually available (*ie* not classified as ground-clutter neither as low-SNR measurements).

The resulting field of filtered radial velocity ($V_{filtered}$) is then taken as the reference field against which raw radial velocity measurements can be compared. The basic assumption behind that methodology is that the radial velocity field can be considered as locally uniform, *locally* meaning over a 5x5 km_ neighborhood. That assumption is certainly not true either close to the radar because of the important variation of the azimuth within the 5x5 km_ square or at high elevation angles because the wind profile is often significantly sheared along the vertical. For those two reasons, the comparison of the set of unfiltered radial velocity measurements (V_1, V_2, V_3, V_{123}, V_{12}, V_{23}, V_{13}) with the filtered velocities is only performed beyond 30 km from the radar and for elevation angles less than 3°.

Figure 2 presents the histogram of the errors on the de-aliased velocity V_{123} in four cases: high-SNR clear-air situation (light grey curve), low-SNR clear-air situation (thick grey curve), convective rain (thin black curve) and all August 2004 (thick black curve). The vertical scale is logarithmic and the range of errors spans [-60; 60] $m.s^{-1}$, which is the Nyquist interval of the de-aliased radial velocity. The bin size of the histograms is 0.25 $m.s^{-1}$. All curves show a well-defined maximum centered on zero: this means that the majority of the radial velocities are properly de-aliased. The histograms, however, are far from being Gaussian: indeed, as already evidenced by Tabary et al. (2005), there are a series of secondary peaks that are distributed quite regularly and symmetrically on either side of the main lobe. Those secondary peaks are without any ambiguity interpreted as de-aliasing errors and they are located at (around)

$\pm 2.k.V_{N1}$, k=1 … 6. The secondary lobes are higher in the low-SNR clear-air case, which means that the amount of de-aliasing failures is more important in that case. This confirms the impression of ruggedness that is given by Fig. 1 (bottom). Whatever curve is considered, the two secondary peaks located at $\pm 2.V_{N1}$ have the largest amplitude, which is at least one order of magnitude smaller than that of the main lobe. Unlike in the dual-PRT case, the amplitude of the secondary peaks does not decrease steadily with increasing error classes. Merely, the secondary peaks at the edges of the spectrum ($\pm 12.V_{N1}$) have the second largest amplitude of all secondary peaks. In other words, the de-aliased velocity is statistically more likely to be in error by $\pm 12.V_{N1}$ (± 60 m.s^{-1}) rather than by $\pm 4.V_{N1}$ (± 20 m.s^{-1}) or $\pm 6.V_{N1}$ (± 30 m.s^{-1}), … The relative amplitude of the secondary peaks is remarkably well reproduced by simulations (see the next Section). It is a direct consequence of the choice of ratios V_{N2} / V_{N1} and V_{N3} / V_{N1}. Another choice of ratio would possibly lead to another distribution of the relative amplitude of the secondary peaks. However, we consider that the distribution is not so important because an error by 10 or 60 m.s^{-1} on the de-aliased velocity amounts exactly to the same, *ie* the measurement is a gross error and cannot be used. To continue on that line of reasoning, the score that is used throughout the paper to evaluate the performance of any dual- or triple-PRT scheme is not the mean error or the Root Mean Square error as it is done usually but the de-aliasing success rate, which is defined as the percentage of velocities that are within $\pm$ 2 m.s^{-1} of the reference velocity. Those scores have been computed for the triple-PRT scheme and for the three dual-PRT sub-schemes. For the triple-PRT scheme, the success rate is 72% in the low-SNR clear-air case, 96% in the high-SNR clear-air case, 90% for the convective rain and 92% for all August 2004. Overall, all scores are acceptable. The triple PRT scheme systematically over-performs any dual-PRT sub-scheme (not shown due to lack of space). In the next section a simulation "à la Zrnic" is used to reproduce the error histograms and revisit the choice of the set of three PRTs.

4. SIMULATION

Figure 3 explains how the simulation of I and Q time series is done in a staggered mode. To simulate a I and Q time series, the Doppler spectrum and the SNR have to be specified. In the following, the SNR value is set to 3 dB and the spectrum is assumed to be Gaussian and therefore only depends upon the mean radial velocity V_r and spectrum width σ_V. The domain over which the spectrum is defined (Nyquist interval $[-V_N;V_N]$) totally determines the time step of the simulated time series ($PRT_{ULTRASHORT}$). The simulation of a staggered time series at PRT_1, PRT_2 and PRT_3 is done by generating a I and Q time series at the shortest possible PRT ($PRT_{ULTRASHORT} << PRT_i$, i=1, 2, 3) and then re-sampling it at the required staggered instants. In the re-sampling process, the I and Q values at a given instant *t* are assigned the values of the ultra-short PRT time series that are the closest in time to *t* (see Fig. 3). As a conclusion, the parameters of the simulation are the following:

- the Gaussian Doppler spectrum P(V) is defined between [–60; 60] m.s^{-1} as follows:

$$P(V) = [\sigma_V\sqrt{(2\pi)}]^{-1} \, . \, exp[-0.5 \, (V\text{-}V_r \, / \, \sigma_V)\_]$$

- 4096 points are used to represent the spectrum;
- the SNR is set to 3 dB;
- the mean radial velocity V_r is assumed to follow the statistical distribution of the median-filtered $V_{filtered}$ velocity obtained for August 2004 (not shown);
- the spectrum width σ_V then appears to be the unique variable parameter of the simulation. Several values of σ_V (1, 2 and 3 m.s^{-1}) have been tested to achieve the best agreement between observed and simulated error histograms.

Figure 4 shows the result of the simulation for the three values of σ_V along with the empirical histogram of August 2004. 10^6 time series have been simulated to produce each histogram. The secondary peaks are remarkably well reproduced both in intensity and location. The magnitude of the secondary peaks decreases when the spectrum width is decreased. For 1m.s^{-1}, only the first-order secondary peaks are visible. The best agreement is obtained for a spectrum width between 1 and 2 m.s^{-1}. The same simulation was carried out with a SNR equal to 10 dB. In that case (not shown) the best agreement was (quite logically) reached for a slightly larger spectrum width (2.5 m.s^{-1}).

The same simulation tool with the same parameters (SNR = 3 dB, σ_V = 1.5 m.s^{-1}, spectrum represented by 4096 points, 10^6 time series simulated) is finally used to exhaustively compare dual versus triple-PRT and to rank the various couples and triplets of PRF in a 2D diagram according to 1) the de-aliasing success rate and 2) the extended Nyquist velocity.
The couples and triplets that have been investigated verify the following conditions :

- PRF_1 (=1/PRT_1) = 379 Hz, 379 Hz being the highest PRF used by the Trappes radar. It can be shown however that the ranking of the different PRT couples or triplets does not change when the highest PRF is increased or diminished under the condition that the other PRF are expressed as a fraction of PRF_1;
- PRF_2 and PRF_3 are not less than PRF_1 / 2 in order not to have too big differences between pulses, which may possibly have detrimental effects on the magnetron. Notice however that the highest PRF (379 Hz) is rather low so that the inequality $\sigma_V << 2V_N$ would certainly not hold below PRF_1 / 2.
- PRF_2 and PRF_3 are expressed as fractions of PRF_1: PRF_2 = (p/q) PRF_1 and PRF_3 = (r/s) PRF_1 with p, q, r and s integers.

- The extended Nyquist velocity of the dual- or triple-PRT scheme should not be larger than 65 $m.s^{-1}$.

In the triple-PRT case, the ratios that are tested are the following: $[V_{N2}/V_{N1};V_{N3}/V_{N1}]$ = [2/3; 4/5], [4/5; 3/5], [3/5;4/7], ... More than 100 possibilities are tested and ranked in a 2D diagram. Due to lack of space, the resulting diagrams are not shown here. Conclusions however are the following :

- At the same extended Nyquist velocity, triple-PRT scheme systematically over-performs dual-PRT.
- For a given extended Nyquist velocity, the best dual-PRT schemes are the ones for which PRF_2 = (p/p+1) PRF_1, which is a classical result.
- For an extended Nyquist velocity of 60 m.s-1, the de-aliasing success rate of the optimal candidate is 90% in triple-PRT and 75% in dual-PRT.
- In the triple-PRT case , the best candidate yielding a Nyquist velocity of 60 $m.s^{-1}$ is $[V_{N2}/V_{N1};V_{N3}/V_{N1}]$ = [6/7; 4/5], ie exactly the one that has been set for the Trappes radar.

5. CONCLUSIONS

A triple-PRT scheme with three low and close to each other PRF(379, 321 and 305 Hz) has been implemented on an operational C-band radar of the French network (Trappes). One month of data comprising clear-air, convective and stratiform rain has been analyzed to evaluate the quality of the de-aliasing procedure. The extended Nyquist velocity is 60 m.s-1. The de-aliasing success rate is beyond 90% except in low-SNR clear-air conditions where it drops down to 76%. The computation of error histograms allows evidencing the de-aliasing failures: they appear as secondary peaks spaced apart by $2.V^{N1}$.
A simulation of staggered I and Q time series “à la Zrnic” has been used to reproduce the observed error histograms. The parameters of the simulation have been set so as to correspond as closely as possible to real measurements conditions. The only free parameter of the simulation is the spectrum width. The best agreement between simulated and observed histograms is obtained when it is set to 1.5 $m.s^{-1}$.
The same simulation tool has been used to exhaustively compare and rank dual and triple-PRT schemes in 2D (de-aliasing success rate and extended Nyquist velocity) diagrams. Triple-PRT systematically overperforms dual-PRT. The best triplet yielding an extended Nyquist velocity of 60 m.s-1 is the one that is in place in Trappes, ie $[V_{N2}/V_{N1};V_{N3}/V_{N1}]$ = [6/7; 4/5].

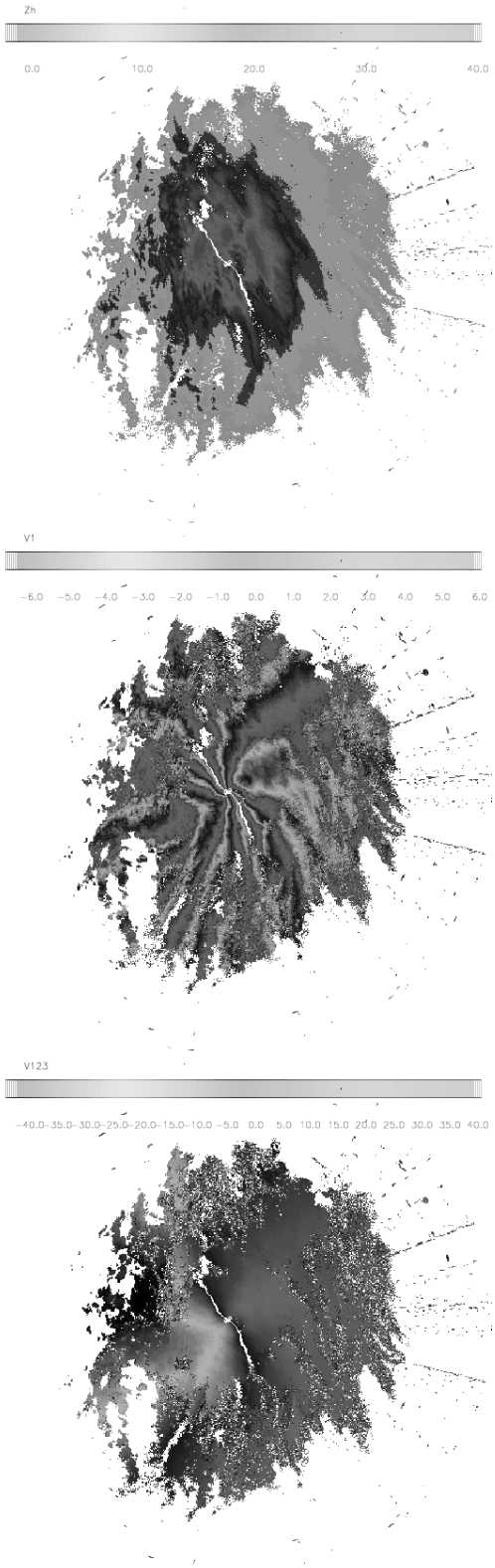

Figure 1 : reflectivity (top), velocity at lag PRT_1 (middle) and dealiased velocity (bottom) for a strong wind case (17 December 2004 10.00 UTC).

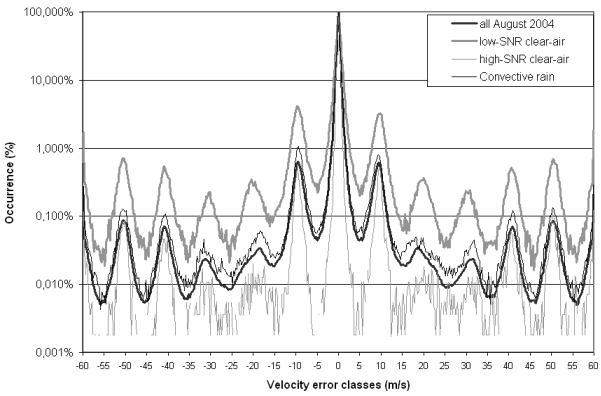

Figure 2 : histogram of errors on the dealiased velocity in four cases (high-SNR clear-air, low-SNR clear-air, rain and all August 2004).

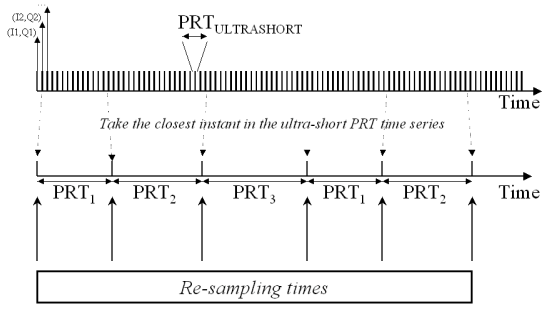

Figure 3 : re-sampling procedure to simulate I and Q time series in any staggered mode.

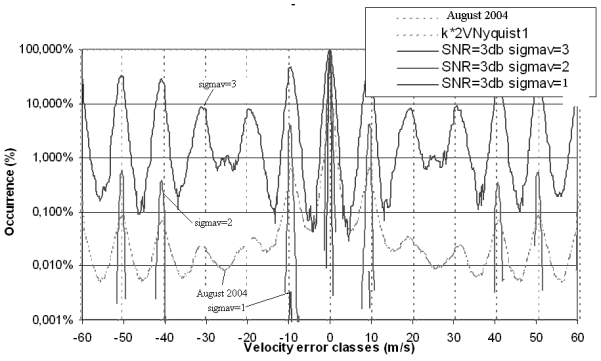

Figure 4 : simulated error histograms for SNR = 3 dB and three values of the Doppler spectrum width (1, 2 and 3 m.s^{-1}).

ACKNOWLEDGEMENTS

This work was done in the frame of the PANTHERE Project (Programme Aramis Nouvelles Technologies en Hydrometeorologie Extension et REnouvellement supported by Météo-France, the French “Ministère de L’Ecologie et du Développement Durable”, the “European Regional Development Fund (ERDF)” of the European Union.

REFERENCES

Sachidananda, M. and D.S. Zrnic, 2002: An Improved Clutter Filtering and Spectral Moment Estimation Algorithm for Staggered PRT Sequences. *J. Atmos. Oceanic Technol.*, 19, No. 12, pp. 2009–2019.

Tabary, P., L. Périer, J. Gagneux and J. Parent-du-Châtelet, 2005: Test of a staggered PRT scheme for the French radar network, *J. Atmos. Oceanic Technol.*, Vol. 22, No. 4, 352 – 364.

Torres, S.M., Y.F. Dubel and D. Zrnic, 2004: Design, Implementation, and demonstration of a Staggered PRET algorithm for the WSR-88D, *J. Atmos. Oceanic Technol.*, Vol. 21, 1389 - 1399.

Zrnic, D. S., 1975: Simulation of weather like Doppler spectra and signals. *J. Appl.Meteor.*, 14, 619–620.

Zrnic, D.S., 1977: Spectral moment estimates from correlated pulse pairs, *IEEE Trans. Aropsp. Electron. Syst.*, AES-13, 344 – 354.

Zrnic, D.S. and P. Mahapatra, 1985: Two methods of ambiguity resolution in pulse Doppler weather radars. IEEE Trans. Aerospace and Electronic Systems, AES 21(4), 470 – 483.

Zrnic, D.S., and A. Zahrai, 2003: Evolution of weather surveillance radars, NSSL’s perspective. Proceedings of the 31st Conference on Radar Meteorology, 6 – 12 Aug. 2003, Seattle, WA, USA.